H ingestion into He-burning convection zones in super-AGB stellar models as a potential site for intermediate neutron-density nucleosynthesis

S. Jones,[1,2]⋆† C. Ritter,[1,3]† F. Herwig,[1,3]† C. Fryer,[4]† M. Pignatari,[5]†
M. G. Bertolli[6,7]†‡ and B. Paxton[8]

[1]*Department of Physics & Astronomy, University of Victoria, PO Bos 3055 Victoria, BC V8W 3P6, Canada*
[2]*Heidelberg Institute for Theoretical Studies, Schloss-Wolfsbrunnenweg 35, D-69118 Heidelberg, Germany*
[3]*Joint Institute for Nuclear Astrophysics, Center for the Evolution of the Elements, Michigan State University 640 South Shaw Lane, East Lansing, MI 48824, USA*
[4]*Computational Physics and Methods (CCS-2), LANL, Los Alamos, NM 87545, USA*
[5]*Konkoly Observatory, Research Centre for Astronomy and Earth Sciences, Hungarian Academy of Sciences, Konkoly-Thege Miklós ut 15-17, H-1121 Budapest, Hungary*
[6]*Physics Division, Oak Ridge National Laboratory, Oak Ridge, TN 37831, USA*
[7]*Department of Physics and Astronomy, University of Tennessee, Knoxville, TN 37996, USA*
[8]*Kavli Institute for Theoretical Physics and Department of Physics Kohn Hall, University of California, Santa Barbara, CA 93106, USA*

ABSTRACT

We investigate the evolution of super-AGB (SAGB) thermal pulse (TP) stars for a range of metallicities (Z) and explore the effect of convective boundary mixing (CBM). With decreasing metallicity and evolution along the TP phase, the He-shell flash and the third dredge-up (TDU) occur closer together in time. After some time (depending upon the CBM parametrization), efficient TDU begins while the pulse-driven convection zone (PDCZ) is still present, causing a convective exchange of material between the PDCZ and the convective envelope. This results in the ingestion of protons into the convective He-burning pulse. Even small amounts of CBM encourage the interaction of the convection zones leading to transport of protons from the convective envelope into the He layer. H-burning luminosities exceed 10^9 (in some cases 10^{10}) $L_\odot$. We also calculate models of dredge-out in the most massive SAGB stars and show that the dredge-out phenomenon is another likely site of convective-reactive H-^{12}C combustion. We discuss the substantial uncertainties of stellar evolution models under these conditions. Nevertheless, the simulations suggest that in the convective-reactive H-combustion regime of H ingestion the star may encounter conditions for the intermediate neutron capture process (i-process). We speculate that some CEMP-s/r stars could originate in i-process conditions in the H ingestion phases of low-Z SAGB stars. This scenario would however suggest a very low electron-capture supernova rate from SAGB stars. We also simulate potential outbursts triggered by such H ingestion events, present their light curves and briefly discuss their transient properties.

Key words: stars: abundances – stars: AGB and post-AGB – stars: evolution – stars: interior.

1 INTRODUCTION

The most important mixing process in stars is convection. One of the least understood aspects of stellar convection is the convective boundary. The way in which convective boundaries are modelled determines many global properties that characterize the evolution of stellar models. In the most simplistic view the convective boundary is given by the Schwarzschild condition ($\nabla_{\rm rad} > \nabla_{\rm ad}$). However, the literal implementation of the Schwarzschild boundary would imply a spherically symmetric composition discontinuity that does not exist in real stars, as shown by hydrodynamic simulations and observations (see e.g. Freytag, Ludwig & Steffen 1996; Schroder, Pols & Eggleton 1997; Deupree 2000; Ribas, Jordi & Gimenez 2000; Herwig et al. 2006, 2007; Rogers, Glatzmaier & Jones 2006; Meakin & Arnett 2007; Woodward et al. 2008; Mocák et al. 2009;

⋆ E-mail: samuel.jones@h-its.org
† NuGrid Collaboration, http://www.nugridstars.org.
‡ Formerly LANL.

Tian, Deng & Chan 2009; Mocák, Muller & Siess 2011; Tkachenko et al. 2014). Numerous strategies have been employed to model the properties of convective boundaries.

Here, we use the simple model of exponentially decaying convective boundary mixing (CBM) initially based on hydrodynamic simulations by Freytag et al. (1996) and first introduced in stellar evolution simulations by Herwig et al. (1997) to address the observational properties of H-deficient post-AGB stars (Werner & Herwig 2006). This or similar exponential models for CBM have been adopted and investigated for many other problems, including the ^{13}C-pocket in low-mass AGB stars (Herwig, Langer & Lugaro 2003; Lugaro et al. 2003; Cristallo et al. 2009a), the observed CNO enhancement of nova ejecta and their fast rise time (Denissenkov et al. 2013a) and the quenching of the C flame in super-AGB (SAGB) stars (Denissenkov et al. 2013b) and the general properties of AGB stellar models (Herwig 2000; Miller Bertolami et al. 2006; Weiss & Ferguson 2009). A quantitative determination of the CBM efficiency in terms of the e-folding distance of the diffusion coefficient by analysis of hydrodynamic simulations has been attempted by Herwig et al. (2007), but the results obtained so far are preliminary because they are based on 2D calculations.

The evolution of SAGB stars is characterized by the ignition of C burning that will lead to the formation of an electron-degenerate ONe core (Garcia-Berro et al. 1994). The details of the outcome of C burning has been shown to depend on the assumptions for convective boundaries. Denissenkov et al. (2013b), Chen et al. (2014) and Farmer, Fields & Timmes (2015) have demonstrated that in models in which CBM is taken into account the C flame is quenched and hybrid CONe white dwarf may form, with numerous possible consequences that impact, for example, upon the progenitor evolution of Type Ia supernovae (Denissenkov et al. 2015; Kromer et al. 2015).

Further burning stages beyond C burning (i.e. Ne, O, Si) are prevented by a combination of electron degeneracy and neutrino cooling. Super-AGB stars may end their lives as ONe (or hybrid CONe; Denissenkov et al. 2013b) white dwarfs or as electron-capture core-collapse supernovae (SNe; Nomoto 1984, 1987; Poelarends et al. 2008; Jones et al. 2013; Doherty et al. 2015). The evolution up to the thermally pulsing SAGB phase is characterized by several dredge-up (DUP) events, including, in some cases, a dredge-out event that brings larger amounts of He-burning products to the surface (e.g. Ritossa, García-Berro & Iben 1999; Siess 2007; Herwig et al. 2012). Since the evolution of the H-shell depends on the abundance of (C+N+O), SAGB thermal pulse (TP) stars that have enhanced C and O abundances because of this dredge-out will afterwards behave as if they had larger initial C+N+O abundances.

The initial mass range for entering the SAGB phase is rather narrow, from $\approx$7.5–9.25 M$_\odot$ at solar metallicity according to Poelarends et al. (2008), 8–9.75 M$_\odot$ according to Doherty et al. (2015) and 7–9 M$_\odot$ according to Woosley & Heger (2015). This result is uncertain as it depends sensitively on the treatment of the H- and the He-core convection boundary. The exact mass range will also depend on the uncertain ^{12}C + ^{12}C nuclear reaction rate. The limiting initial mass for C ignition decreases from about 7.1 M$_\odot$ to about 5.4 M$_\odot$ when the C-burning rate is increased from $0.1\lambda_{CF88}$ to $1000\lambda_{CF88}$ (Chen et al. 2014), where λ_{CF88} is the rate from Caughlan & Fowler (1988). This corresponds to a decrease in the limiting core mass from 1.1 to 0.93 M$_\odot$. At lower metallicity the mass range for the formation of SAGB stars will span lower initial masses (see e.g. Siess 2007).

The composition of the wind ejecta and evolutionary fate of SAGB stars at low metallicity is of particular importance for the interpretation of multiple populations observed in some globular clusters, in particular the He-rich blue main sequence in Ω Cen (Anderson 1997) and several other clusters. These second (or third) generation populations have also unusual C, N and O abundances and models of SAGB stars (e.g. Ventura & D'Antona 2011; Herwig et al. 2012; Karakas, Marino & Nataf 2014) have been used to address the abundance anomalies of distinct populations in globular clusters. Herwig et al. (2012) have proposed the Galactic plane passage gas purging chemical evolution scenario to integrate photometric and stellar evolution information with dynamic constraints from the cluster's orbit to address many of the observed abundance properties of the distinct populations in Ω Cen. In this work we are reporting on further, and more detailed investigations of the SAGB phase in stellar models.

Different groups using different stellar evolution codes obtain reasonably similar results for the SAGB evolution if the same assumptions (in particular for mixing) are made (Poelarends et al. 2008; Siess 2010; Doherty et al. 2010, 2014). While some of these studies go beyond the strict Schwarzschild criterion for convection, none of these previous investigations have, to our knowledge, explored the effect of variable CBM efficiencies.

The effect of CBM in low-mass AGB stars has been investigated in detail via simple CBM algorithms which effectively model a mixing diffusion coefficient that exponentially decreases with geometric distance from the convection boundary (Herwig et al. 1997; Mazzitelli, D'Antona & Ventura 1999; Herwig 2000; Miller Bertolami et al. 2006; Weiss & Ferguson 2009). The consequences of CBM for He-shell flash convection are larger ^{12}C and ^{16}O abundances in the intershell, in agreement with observations of H-deficient post-AGB stars (Werner & Herwig 2006), and larger peak temperatures for the ^{22}Ne-fuelled *s*-process contribution. Lugaro et al. (2003) have argued that this may lead to isotopic ratio predictions, for example for Zr, that could be incompatible with observations from pre-solar grains. This question needs to be revisited however, considering possible modifications to the details of the mixing algorithm as well as the latest nuclear reaction rate data, in particular for the ^{22}Ne(α, n)^{25}Mg neutron source reaction rate (e.g. Longland, Iliadis & Karakas 2012; Bisterzo et al. 2015) and Zr neutron capture rates (Liu et al. 2014; Lugaro et al. 2014). Denissenkov et al. (2013a) have shown that with exponential-diffusive CBM the observed enhancement of C and O in nova ejecta and the fast rise time of the nova light curve can be reproduced in 1D models. CBM has been reported in multidimensional simulations of nova shell flashes (Casanova et al. 2011; Glasner, Livne & Truran 2012). It is also accepted that CBM in the form of some sort of overshooting prescription needs to be employed during the core H-burning phase on the main sequence, and almost all stellar evolution calculations do account for this convection-induced extra mixing.

Rotationally induced mixing at the bottom of the convection zone has been shown to be insufficient in spherically symmetric simulations (Herwig 2003; Siess, Goriely & Langer 2004) to model the partial mixing between the H-rich envelope and the ^{12}C-rich core that leads to the formation of the ^{13}C-pocket in low-mass AGB stars (e.g. Herwig 2000; Cristallo et al. 2009b). In addition, it may reduce significantly the *s*-process yields (Piersanti, Cristallo & Straniero 2013). How well rotationally induced mixing can be approximated in one-dimensional models of stars is unclear at present.

Thus, there is significant motivation to investigate how the evolution of SAGB stars proceeds if small and moderate efficiencies of CBM are taken into account at all convective boundaries. In the case of SAGB stars, this makes the computations numerically much more demanding, and in many cases the quantitative details of the results have to be considered as very uncertain. This is so because (i) the exact amount and efficiency of CBM is presently unknown for the convection boundaries in SAGB stars, and (ii) we frequently encounter in these calculations of convective-reactive H-combustion regimes that at least locally violate some of the assumptions that are the basis of 1D spherically symmetric stellar evolution codes with the mixing-length theory for convection (MLT). In that sense, the computations presented here are in a way to be considered as a road map which points out areas in which more detailed 3D hydrodynamic investigations need to be performed in the future.

In this paper, we report on the occurrence of convective-reactive H-combustion flashes in SAGB TPs in stellar models when CBM is included. These H ingestion flashes present specific differences from H ingestion flashes found previously in normal AGB stars of very low metallicity (e.g. Fujimoto, Ikeda & Iben 2000; Herwig 2003; Suda et al. 2004; Campbell & Lattanzio 2008; Cristallo et al. 2009a). In particular, the latter are usually a one-off event which removes, through copious DUP of C and O, the conditions for its occurrence. The H-combustion flashes we observe in SAGB stars can be recurrent as they are initiated after the peak He-burning luminosity of each shell flash as a result of a very fast and efficient DUP while the He-shell is still convective. Nevertheless, the nucleosynthesis processes following the ingestion are expected to be quite similar, being driven by a fast burning of protons and by the consequent formation of ^{13}C.

The ^{13}C made by H-^{12}C combustion activates the ^{13}C(α, n)^{16}O reaction, producing an intermediate neutron density of $N_n \approx 10^{15}$ cm^{-3}, defined as the *i-process* by Cowan & Rose (1977). We adopt this designation for all n-capture regimes driven by convective burning of protons in He-burning convection zones. Such conditions can be found in numerous stellar environments, particularly in stars of very low metallicity, such as the He-core flash in low-metallicity stars (Campbell, Lugaro & Karakas 2010).

As shown recently by Herwig et al. (2011) 1D stellar evolution simulations with MLT do not predict surface observed abundances of the post-AGB H ingestion star Sakurai's object. Instead, alternate mixing assumptions had to be made for that reactive-convective event, based on its hydrodynamic nature. Recent attempts of hydrodynamic simulations of the H ingestion event in Sakurai's object have shown a much more violent behaviour than expected from stellar evolution models, and led to the discovery of the global oscillation of shell-H ingestion (GOSH; Herwig et al. 2014). The GOSH is a non-radial instability that develops out of a spherically symmetric initial state, and rearranges the internal stratification in ways that would have been impossible to predict based on stellar evolution simulations alone. The GOSH simulations of Herwig et al. (2014) only cover a first non-radial instability which is likely to be followed by further violent and non-radial hydrodynamic events. Validated sub-grid models for reactive-convective regions to be employed in stellar evolution models are therefore not yet available, and thus we have to consider stellar evolution results as uncertain once the convective-reactive phases are occurring.

With these caveats in mind, we will briefly present the physics assumptions for our simulations in Section 2. In Section 3, we describe the main results. In Sections 4 and 5, we discuss the potential consequences of our results.

2 METHOD

2.1 Stellar evolution code and physics assumptions

For the stellar evolution simulations presented here we use the MESA code (Paxton et al. 2011, 2013, 2015).[1] The MESA papers by Paxton et al. already contain verification cases for a wide range of stellar evolution scenarios, including TPs and DUP in AGB stars. In addition, we have now also run massive AGB models with the same initial abundances and similar enough physics assumptions as those chosen for the grid of models including massive AGB stars by Herwig (2004a) obtained with the EVOL stellar evolution code, and we find the MESA results again to be in good agreement.

We use a custom nuclear network with 31 species – based on the MESA network agb.net – including the major isotopes for elements from H to Al and closing with ^{28}Si. For reactions we included PP-chains, CNO cycles, the NeNa and MgAl cycles, $3\alpha \rightarrow {}^{12}$C, ^{12}C($\alpha$, γ)^{16}O, ^{13}C(α, n)^{16}O, and ^{12}C + ^{12}C (both α and p exit channels), amongst other less critical reactions. Although we included the ^{13}N isotope explicitly we did not include the ^{13}N(p, γ)^{14}O reaction, which would have been relevant. However, this omission will not change any of the main findings, and will be corrected along with several other approximations to the network in a forthcoming more detailed nucleosynthesis investigation of these models. Reaction rates are taken from the NACRE compilation (Angulo et al. 1999).

MLT is employed to calculate the temperature gradient in the convective regions and predict the convective velocities. Mixing in convective regions is approximated as a diffusive process with diffusion coefficient $D = \frac{1}{3}v\alpha_{MLT}H_P$, where v is the convective velocity according to MLT and H_P the scaleheight of pressure. For the mixing-length parameter we adopt $\alpha_{MLT} = 1.73$. In addition to the default mesh controls we refine the mesh on the abundances of H, ^{4}He, ^{13}C and ^{14}N. Additional criteria are added to resolve He-shell flashes and the advance in time of the thin H-burning shell during the interpulse phase. We use the atmosphere option 'simple_photosphere', which gives the surface pressure as

$$P_s = \frac{2GM}{3\kappa_s R^2} \left[1 + 1.6 \times 10^{-4} \kappa_s \left(\frac{L/L_\odot}{M/M_\odot} \right) \right] \quad (1)$$

(see Paxton et al. 2011 and Cox & Giuli 1968, Section 20.1). κ_s is the surface opacity, for which an initial guess is made and converged iteratively with the pressure. We assume a mass-loss rate of $\log(\dot{M}/ M_\odot \text{ yr}^{-1}) \approx -4.8$ which is obtained by using the Blöcker (1995) mass-loss rate in MESA with $\eta = 5 \times 10^{-4}$. This is likely to be at the low end of a rather uncertain range of possible mass-loss rates for these stars. We adopt the OPAL C- and O-enhanced opacities in MESA (Iglesias & Rogers 1996).

2.2 Convective boundary mixing

We have discussed CBM and some evidence from hydrodynamic simulations in the Introduction. Note that we are avoiding the term overshooting and instead prefer to describe a wide range of hydrodynamic instabilities that can be observed at and near convective boundaries as CBM. A variety of fluid dynamics processes and hydrodynamic instabilities can contribute to CBM, such as buoyancy-driven overshooting of coherent convective systems (Freytag et al. 1996), Kelvin–Helmholtz instabilities (Meakin & Arnett 2007;

---

[1] Details about the versions of the MESA code that were used will be made available online along with the inlists.

Casanova et al. 2011) which in turn may be enabled by boundary-layer separation (Woodward, Herwig & Lin 2015), or mixing due to internal gravity waves (Denissenkov & Tout 2003).

As we described in the Introduction, our stellar evolution simulations approximate abundance mixing due to these CBM processes – no matter what their physical origin is – via the exponentially decaying mixing algorithm described in Freytag et al. (1996) and first applied in stellar evolution calculations by Herwig et al. (1997). In this approximation, the diffusion coefficient takes the form

$$D_{CBM} = D_0 \exp\left(-\frac{2|r - r_0|}{f H_P}\right), \qquad (2)$$

where H_P is the pressure scaleheight and D_0 is the diffusion coefficient given by MLT at a location r_0. f is a parameter defining the e-folding length $f H_P$ of the diffusion coefficient.

D_0 is not defined at the convective boundary because in MLT, the convective velocity is zero there. Instead of taking D_0 at the last convective zone, the MESA implementation allows us to specify how far inside the convection zone from the boundary the exponential decay should begin. The Eulerian coordinate of this location is then r_0. Indeed, the results of Freytag, Ludwig & Steffen (1996, their figs 10 and 14) and Herwig et al. (2006, their fig. 24) show that the decay of the radial component of the convective velocity and of the inferred radial diffusion coefficient begins inside the convective zone and not at the formal convective boundary. In the MESA implementation, there is a second parameter for each convective boundary f_0, which specifies how far from the convective boundary, on the convective side, the decay should begin. This distance is $f_0 H_P$. In our models, we use $f_0 = f$ at all convective boundaries. The diffusion coefficient as formulated in equation (2) is then applied in the direction of the convective boundary and across into the stable layer.

The value of f has no direct, simple and intuitive relation to the physical flow properties – other than larger values indicate more efficient and more spatially extended mixing than smaller values – because it is a number that, when multiplied by the local scaleheight of pressure, gives the e-folding length of the diffusion coefficient that is representing mostly non-diffusive mixing processes caused by a variety of hydrodynamic processes.

For our benchmark model, we have assumed $f = 0.014$ at all convective boundaries (including the H- and He-core burning phases), except at the bottom of the convective envelope (including during the third dredge-up, TDU, if it occurs) where we assume $f_{env} = 0.0035$, and at the bottom of the pulse-driven convection zone (PDCZ) where we assume $f_{PDCZ} = 0.002$. The values of f_{env} and f_{PDCZ} are lower by a factor of about 36 and 4, respectively, compared to what we usually assume in our low-mass AGB simulations (which generally agree with observations in post-AGB H-deficient stars and planetary nebulae; e.g. Werner & Herwig 2006; Pignatari et al. 2013a; Delgado-Inglada et al. 2015) and compared to what has been shown to reproduce observational characteristics of nova shell flashes (Denissenkov et al. 2013a). As discussed previously by Herwig (2004) and Goriely & Siess (2004), DUP may be *hot* in (super-) AGB stars of low metallicity and larger initial mass, where the H-burning at the bottom of the convective envelope can become important already during the DUP phase. Another way to look at it is that the familiar hot-bottom burning already starts during the TDU in AGB stars of low metallicity and larger initial mass. As discussed briefly by Herwig (2004), a larger CBM efficiency during the DUP phase in massive AGB or SAGB stars may result in the formation of a corrosive H-burning flame that may terminate the AGB through enhanced mass-loss.

When hydrogen is burning at the bottom of the convective envelope, the boundary will be stiffer (lower CBM efficiency) because of the entropy barrier produced in the vicinity of the burning shell. Unfortunately, without detailed hydrodynamics simulations or fluid experiments, it is difficult to know how much stiffer the boundary becomes. In addition, translating such a stiffness into a CBM parameter f_{env} is not straightforward. The choice of $f_{PDCZ} = 0.008$ below shell-flash convection zones on top of degenerate cores is a good starting point, with a similar value being able to reproduce the intershell abundances of post-AGB stars and the ejecta enrichment and fast light curve rise times of novae (Werner & Herwig 2006; Denissenkov et al. 2013a). However, the conditions in the shell flashes of SAGB stars, post-AGB stars and novae are certainly not identical. For example, in post-AGB stars the peak luminosities are higher than those in SAGB stars by roughly an order of magnitude. Furthermore, the stiffness of the convective boundaries and the aspect ratio of the convection will naturally also vary from site to site. The correlation of CBM efficiency with nuclear energy generation rate or driving luminosity of the convection is no easy task and requires detailed, targeted study. For these reasons, we study a range of values for f_{env} and f_{PDCZ} in the present work with a view to motivating such targeted studies.

Again, the details will depend critically on the assumed mixing properties at the convective boundaries which need to be investigated eventually by means of three-dimensional stellar hydrodynamics simulations. We address this uncertainty by providing a parameter study of the dependence of our H ingestion results on the CBM parameters. As we will describe in Section 3, H ingestion in our TP-SAGB models is highly sensitive to CBM at the base of the PDCZ and at the base of the hot-bottom-burning H-envelope during TDU. These affect the response time or rate of the DUP as well as its depth (see Mowlavi 1999; Herwig 2004). The CBM *above* the PDCZ, which is a critical factor in the H ingestion He-shell flashes of low-metallicity AGB stars and very late thermal pulses (VLTPs) in post-AGB stars, is of less importance here. Indeed, we have computed models with a range of CBM efficiencies above the PDCZ and it is clear that this CBM does not initiate an H ingestion TP in our TP-SAGB models unless unjustifiably high efficiencies are used. The overshoot at the top of the PDCZ has been studied by Herwig, Blöcker & Driebe (2000), who also find no significant impact of this CBM on the proximity of the PDCZ to the convective H envelope. Thus, we limit our parameter study to only f_{env} and f_{PDCZ}.

3 STELLAR EVOLUTION MODELS

The evolution up to the beginning of the TP phase proceeds in a similar manner to that described in previous studies (e.g. Ritossa et al. 1999; Siess 2007; Doherty et al. 2010; Ventura & D'Antona 2011; Jones et al. 2013). The abundance signature of the early AGB during the second DUP is a significant enhancement of He to a mass fraction of about 0.37. This is followed in the more massive SAGB models by a 'dredge-out' after the carbon shell burning episodes, which can be considered as another DUP event following an initial convective He-shell burning episode that precedes the regular TPs. This mixing event brings large amounts of C and O to the surface (see e.g. Ritossa, García-Berro & Iben 1999; Siess 2007; Herwig et al. 2012, and Section 3.1).

Afterwards, the bottom of the convective envelope continues to corrosively penetrate further into the He-burning ashes and the H-free core is reduced by an additional $\Delta m_r \approx 10^{-2}\,M_\odot$. This last DUP phase before the onset of regular TPs is facilitated by

CBM. As described in Herwig (2004), H is mixed into a very thin layer below the Schwarzschild convective boundary and generates there H-burning luminosities of the order of $\log L_H/L_\odot \approx 5.5$. This mixing-induced H-flame will continue until the conditions for DUP are removed, i.e. the excess energy from previous nuclear flashes and core contraction has escaped the envelope. However, in view of preceding and following mixing and burning events, this short phase of H-flame core penetration does not have a large effect, except that the transformation of C and O into ^{14}N is starting during this phase, but only getting fully underway during the following TP phase.

3.1 H-^{12}C combustion during dredge-out

The most massive SAGB stars and failed massive stars (Jones et al. 2013) experience a dredge-out event (Ritossa et al. 1999; Siess 2007; Doherty et al. 2015). This is when shell helium burning releases enough energy to induce convection during the second DUP, as mentioned briefly above. A combination of the release of gravothermal energy and of nuclear energy cause the helium-shell convection zone to grow (outwards) in mass and merge with the descending base of the convective hydrogen envelope (Fig. 1). There are three main reactions contributing to the nuclear energy generation during this phase: ^{12}C + ^{12}C, ^{12}C$(\alpha, \gamma)^{16}$O and the triple-α reaction. The energy sources are physically stratified in only a very thin (roughly 3×10^{-2} M$_\odot$) mass shell (see Fig. 2).

The two main consequences of dredge-out are the enrichment of the envelope with ashes of hydrogen burning and incomplete He burning, and the advection of protons down to He-burning temperatures where primary ^{12}C is present with a typical mass fraction of $X(^{12}$C$) \approx 0.5$. A strong flash occurs as the protons are mixed rapidly into the hotter layers below the base of the H envelope. This has previously been reported by Gil-Pons & Doherty (2010), who found that the resulting hydrogen burning produced local luminosities in excess of 10^6 L$_\odot$. As we will describe here our models suggest that in rapid combustion of the H with ^{12}C local luminosities well in excess of 10^9 L$_\odot$ may be reached.

The dredge-out event is illustrated in Fig. 1 for a 7.5 M$_\odot$ $Z = 10^{-3}$ model (top panel) and for a 8.4 M$_\odot$ $Z = 0.01$ model (bottom panel). In this simulation the strict Schwarzschild criterion (i.e. no CBM) is assumed at the lower boundary of the convective envelope. Our simulations confirm that dredge-out is encountered without CBM at the lower boundary of the convective envelope. Dredge-out has been reported and described also by, e.g. Ritossa et al. (1999), Siess (2007), Gil-Pons & Doherty (2010) and Doherty et al. (2015), none of whom prescribe for CBM (though each group has their own method of treating the convective boundary). We have simulated massive SAGB and failed massive stars with initial metallicities between $Z = 10^{-5}$ and 0.02, and dredge-out is seen to occur at all metallicities when holding our CBM assumptions described in Section 2.2 *and* when setting $f_{env} = 0$.

During the dredge-out, protons are mixed down through the helium shell towards higher temperatures. In the 8.4 M$_\odot$, $Z = 0.01$ model the protons reach temperatures in excess of 2×10^8 K, where their fraction by mass is a few 10^{-6}. The energy generation at this location reaches a few 10^{13} erg g^{-1} s^{-1}. The abundance profiles, temperature stratification and specific nuclear energy generation at the time of peak nuclear energy generation are shown in Fig. 3 and these characteristics are summarized again in Table 1.

In order to characterize the dynamic importance of the convective-reactive nuclear energy release, we introduce a dimensionless number which relates the nuclear energy released to the
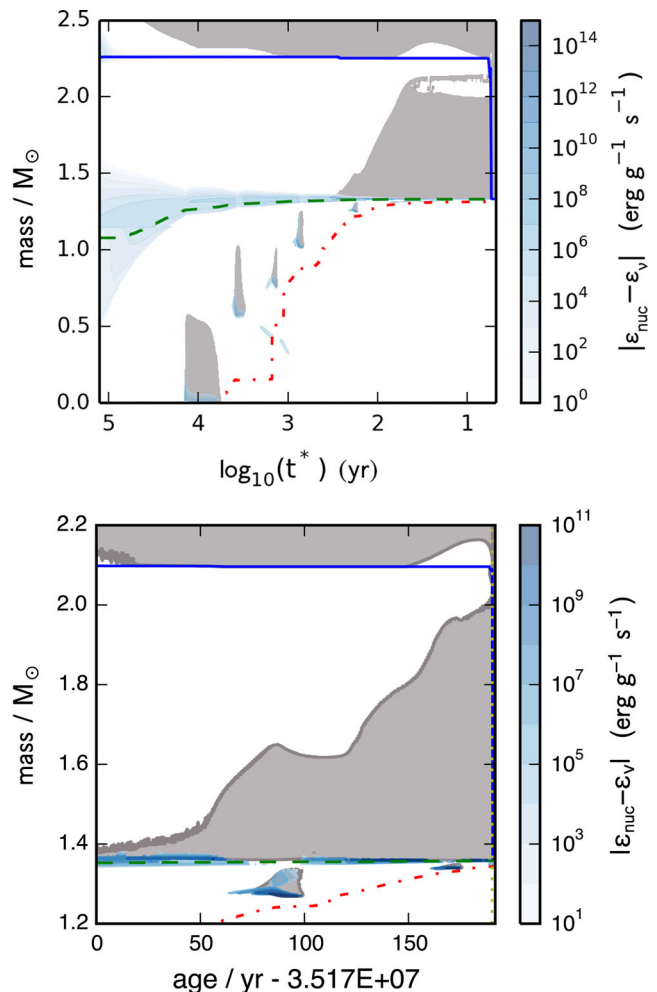

Figure 1. Top panel: evolution of the convective structure and energy generation during dredge-out in a 7.5 M$_\odot$ $Z = 0.001$ stellar model. t^* is the time remaining until the end of the calculation. Grey regions are convectively unstable according to the Schwarzschild criterion, while white regions are stable. The solid (blue), dashed (green) and dot–dashed (red) lines indicate the H-free, He-free and C-free core boundaries, respectively. A convective layer develops in the He shell and grows outwards in mass towards the base of the descending convective envelope. Eventually, the two coalesce and protons are mixed down to the bottom of the He-burning shell on a convective turnover time-scale. Bottom panel: same as top panel but for the 8.4 M$_\odot$ $Z = 0.01$ model as a function of time, zoomed in.

internal energy. As protons are advected into the He-shell convection they will encounter increasing temperature and primary ^{12}C with mass fraction well above 10 per cent. A large amount of nuclear energy is released on the convective advection time-scale via the ^{12}C$(p, \gamma)^{13}$N reaction (see appendix A.2 in Herwig et al. 2011). The fastest time-scale on which this energy can escape under the assumption of hydrostatic equilibrium is the convective turn-over time. Thus, the product $\epsilon_{nuc}\tau_{conv}$ is here an estimate of the nuclear energy from convective-reactive H combustion that will accumulate in the combustion flame. We define

$$H = \frac{\epsilon_{nuc}\tau_{conv}}{E_{int}}, \tag{3}$$

where ϵ_{nuc} is the specific energy generation from nuclear reactions, τ_{conv} is a mixing time-scale and E_{int} is the specific internal energy of the stellar material. For the mixing time-scale, using the scale-height of pressure at the base of the convective He-burning shell
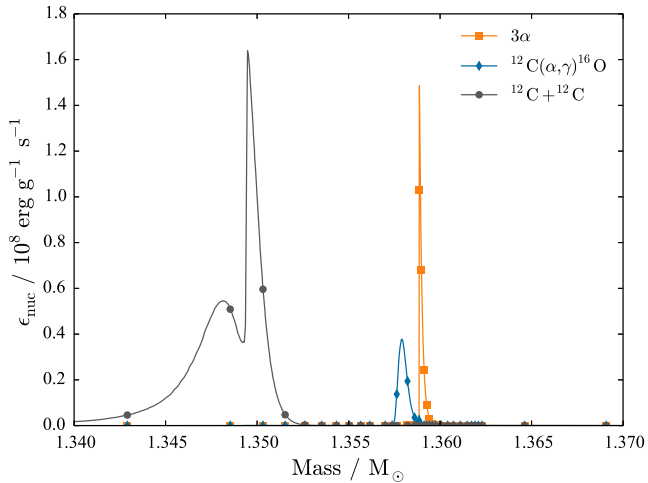
Figure 2. Stratification of the three predominant energy-generating nuclear reactions during the dredge-out phase in the $8.4\,M_\odot$ $Z = 0.01$ model from Fig. 1 (bottom panel) at a time from the right-hand side of the plot where the yellow dotted line is drawn.

Table 1. Characteristic conditions during H ingestion in both dredge-out and TP-SAGB sites.

Site	$T\,/\,K$	$\rho\,/\,\mathrm{g\,cm^{-3}}$	X_H	X_C
dredge-out	$\sim 2 \times 10^8$	$\sim 2 \times 10^2$	$\gtrsim 10^{-6}$	$\sim 10^{-2}$
TP-SAGB	$\sim 2 \times 10^8$	~ 60	$\sim 3 \times 10^{-2}$	~ 0.2

($H_P \approx 1000\,\mathrm{km}$) as a length scale and the *maximum* convective velocity predicted by MLT inside the helium-burning shell ($v_{\mathrm{conv}} \approx 3\,\mathrm{km\,s^{-1}}$), we find a lower limit of

$$\tau_{\mathrm{conv}} \approx \frac{H_P}{v_{\mathrm{conv}}} = 409\,\mathrm{s}. \tag{4}$$

With these assumptions $H = 0.11$. This means that in the combustion flame layer the cumulative nuclear energy input is of the order of 11 per cent of the internal energy, or 8 per cent of the binding energy of the layer, or greater.

The H-number estimate suggests that the H ingestion may release and add to the flow a significant fraction of the binding energy of the layer, in which case fundamental assumptions of stellar evolution, such as hydrostatic equilibrium and the applicability of MLT become inappropriate. Herwig et al. (2011) have shown that in another case of convective-reactive H ingestion observations cannot be reproduced with MLT/stellar evolution models. Sakurai's object
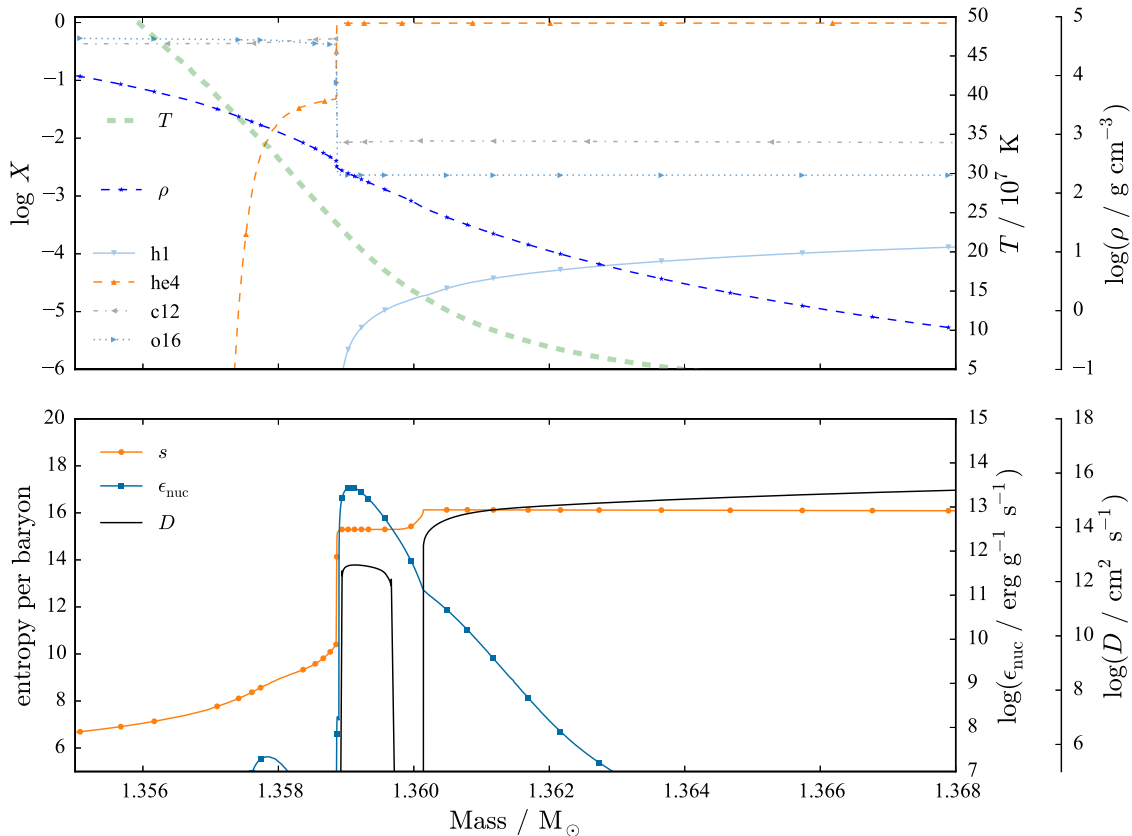

Figure 3. Abundance profiles with the temperature and density stratification (top panel), entropy s, specific energy generation rate and diffusion coefficient (bottom panel) in the $8.4\,M_\odot$ $Z = 0.01$ model during the peak energy generation due to H-^{12}C combustion (very right-hand side of Fig. 1, bottom panel, where the solid blue H-free core boundary penetrates down to the green dashed He-free core boundary, indicated by a vertical dotted yellow line). The points are illustrative and do not reflect the grid. At the base of the convective helium layer (just below mass coordinate $1.360\,M_\odot$), the mass fraction of protons is a few 10^{-6} and the temperature is in excess of 2×10^8 K. These are precisely the conditions under which the neutron densities characteristic of the *i*-process can be achieved due to the release of neutrons in the $^{12}\mathrm{C}(p, \gamma)^{13}\mathrm{N}(\beta^+\nu)^{13}\mathrm{C}(\alpha, n)^{16}\mathrm{O}$ reaction chain. In our 1D hydrostatic simulations, the protons burn as they are transported inwards through regions of increasing temperature. The burning taking place at mass coordinate $M_r \approx 1.360\,M_\odot$ increases the entropy and causes a split in the convection zone, which can be seen as a break in the diffusion coefficient profile.

is a VLTP object with a 2-dex enhancement of first-peak n-capture elements. Only by adopting significant modifications to the MLT mixing predictions could nucleosynthesis simulations reproduce the observations. Herwig et al. (2014) presented hydrodynamic simulations of the H ingestion event in Sakurai's object and reported a non-radial GOSH for a situation similar to the one encountered here for the H ingestion during the dredge-out. We therefore conclude in a similar manner that these stellar evolution models with MLT, and estimates such as the *H*-number based on these models, are not entirely realistic once the H ingestion event with a large *H*-number occurs.

The peak energy generation due to H-^{12}C combustion during the dredge-out is short-lived in our MLT stellar evolution models. The burning of protons as they are transported inwards modifies the entropy structure of the region of interest. The entropy and diffusion coefficient profiles are shown in Fig. 3. In the stellar evolution model, the entropy produced by the burning of hydrogen causes a split in the convection zone, resulting in two convective regions that do not mix further. The protons in the lower convective zone are quickly destroyed, after which fresh hydrogen brought down is burned at the top of the split. There, the temperature is only $\approx 1.5 \times 10^8$ K but nevertheless a few 10^{-3} in mass fraction of ^{13}C is produced. A split in the diffusion coefficient under similar conditions was seen in the models of Herwig et al. (2011). The authors found that the basic assumptions that contribute to the formation of the split – such as a spherically symmetric H-abundance and a spherically symmetric inward diffusion of H – were not found in three-dimensional hydrodynamic simulations. Hence the hypothesis that two convective regions should mix to some extent.

This modified mixing assumption by Herwig et al. (2011, whereby the two convection zones split by the formation of the entropy barrier due to H-burning are allowed to continue to mix) leads to n-capture nucleosynthesis at neutron densities of $N_n \approx 10^{15}$ cm^{-3}. This is approximately two orders of magnitude higher than in the highest neutron densities encountered in the *s*-process powered by the ^{22}Ne neutron source in the He-shell flash convection zone of massive AGB stars (see e.g. Straniero, Cristallo & Piersanti 2014, their table 1). This n-capture regime has been labelled the intermediate regime, or *i*-process by Cowan & Rose (1977). We propose that the H ingestion induced hydrodynamics in the SAGB dredge-out He-burning convection zone would behave similarly to the situation investigated for the H ingestion event in Sakurai's object, in the sense that further mixing between the convection zones will lead in a similar way to the copious production of ^{13}C and the associated intense neutron burst (see e.g. Lugaro, Campbell & de Mink 2009; Campbell et al. 2010). This hypothesis will need to be tested by appropriate hydrodynamic simulations. In the meantime, based on the evidence available at this time we adopt as the most likely scenario that the dredge-out in SAGB stars is a site for *i*-process nucleosynthesis (see Section 4).

In failed massive stars that would become electron-capture SNe, the dredge-out occurs about 30 yr before the explosion. With hydrodynamics simulations suggesting that the flow of protons into the He-burning layer should persist it is entirely possible that enough energy is released in the ingestion to unbind and eject material that has been exposed to such large energy generation rates. Without detailed multiphysics simulations, it is very difficult to know to what extent energy is dissipated during the ingestion/ejection event, but nevertheless we entertain this possibility and examine it in more detail in Section 4.2, where we also predict what the light curve of such a transient might look like.

Table 2. Summary of the models presented here as a metallicity study. These models assume $f_{env} = 0.0035$ and $f_{PDCZ} = 0.002$ (see text for details). M_C^{SAGB} is the mass of the H-free core at the first TP. Also given is whether or not a H ingestion TP is encountered and if so, the peak H-burning luminosity is given.

Z	$M_{ini}/$M$_\odot$	M_C^{SAGB}	H ing?	peak $L_H/10^9$ L$_\odot$
0.02	8.2	1.26975	N	–
0.01	8.15	1.28025	N	–
10^{-3}	7.0	1.24606	Y	8.25
10^{-4}	7.0	1.26263	Y	8.26
10^{-5}	7.2	1.27432	Y	8.48

3.2 TP-SAGB models and TP evolution

We have calculated TP-SAGB models with initial metallicities of $Z = 0.02$, 0.01, 10^{-3}, 10^{-4} and 10^{-5} (Table 2). These models were computed holding the input physics assumptions described in Section 2.2. The TP properties are sensitive to the core mass, and therefore the initial masses were chosen such that the CO core masses of all the models at the first TP were similar (the standard deviation in the CO core masses at the first TP is 0.012 M$_\odot$; see Table 2).

The purpose of this metallicity survey in the models is to compare the TP properties of the SAGB models at different metallicities with regards to approaching the conditions for a H ingestion event to take place. H ingestion occurs in our TP-SAGB models, as we will show, when the TDU (the deepening of the convective envelope in mass following the TP; see Fig. 4), facilitated by CBM, reaches into the PDCZ. In order for this to happen, the TDU must be rapid enough, and deep enough, to cause a convective exchange of material between the convective H-envelope and the PDCZ.

A TDU event regularly follows each He-shell flash although is often absent for the first few flashes. As the models evolve along the TP-SAGB, the time Δt between the extinction of the PDCZ t_1 and the beginning of the TDU t_2 becomes shorter (see definitions in the illustration in Fig. 4). This trend is seen for models at all metallicities that we have considered and is shown in Fig. 5 (top panel, see also Mowlavi 1999 and Herwig 2000). We define the beginning of the TDU in these models as the time when the base of the convective envelope has deepened in mass by 1 per cent of ΔM_{DU} for a given TDU. Of particular note is the result that after about 10–15 pulses (depending on the initial metallicity) the TDU starts while the PDCZ is still active, with the lower metallicity models reaching this point earlier in the TP-SAGB. In this case $\Delta t < 0$ (Fig. 5, top panel), which is one of the criteria for hydrogen from the envelope to be ingested into the PDCZ. If Δt were always positive then the kind of ingestion that we describe here, where the hot TDU reaches the PDCZ, could never happen. Even if we do not always see explicitly the H ingestion in 1D models, one of the main conditions for this to happen – i.e. the TDU beginning already at the time when the PDCZ is still active – is given robustly after at most 16 TPs at all initial metallicities for which we have computed models (Table 2 and Fig. 5, top panel).

The TDU efficiency λ is defined as the ratio of dredged-up mass ΔM_{DU} to core-growth ΔM_H since the end of the previous TDU (see e.g. Lugaro et al. 2003, and Fig. 4). In our models TDU is not always deep enough to mix He-burning products to the surface (i.e. ΔM_{DU} is not always larger than ΔM). For $\Delta M_{DU} < \Delta M$, neither does the model experience a H ingestion TP.

λ is consistently higher for the models with $Z \leq 10^{-3}$ than higher Z models for a similar pulse number. In fact, the models with
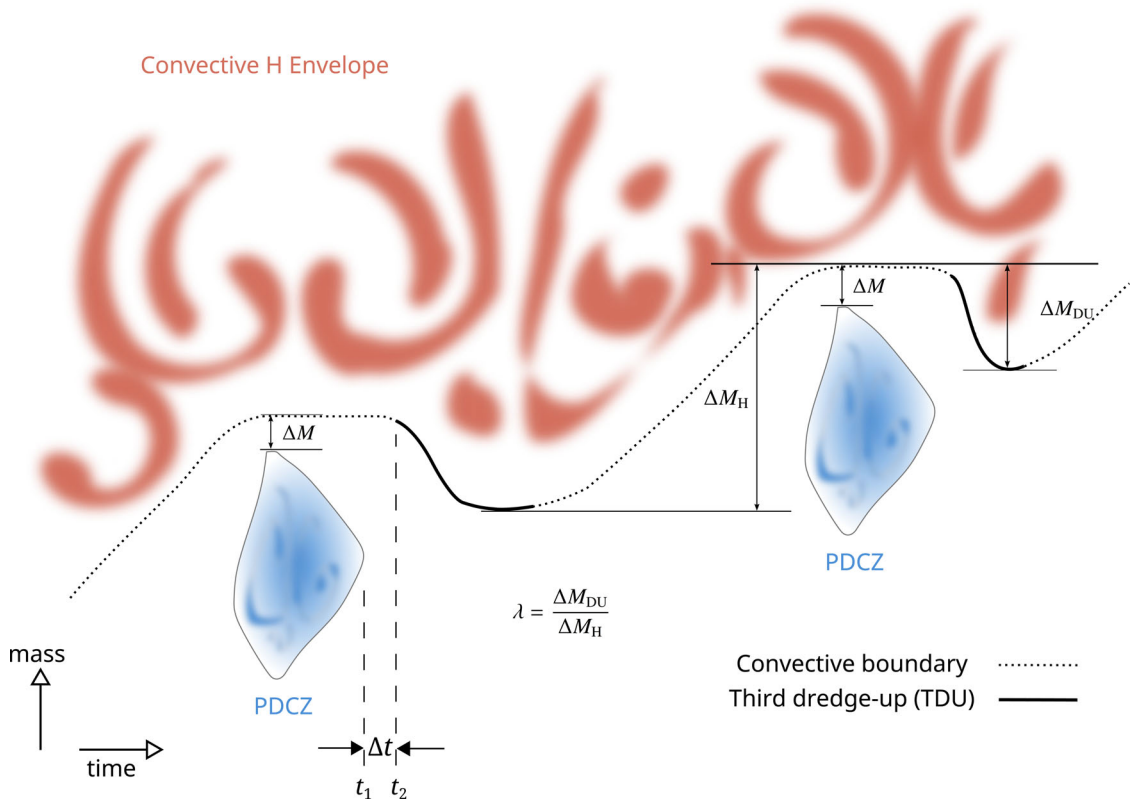
Figure 4. Illustration of the TP-SAGB phase, defining the PDCZ, the convective envelope base penetration (CEBP), t_1 and t_2 – the times of PDCZ extinction and beginning of CEBP, respectively – and the time interval between t_1 and t_2, Δt.

$Z \leq 10^{-3}$ all experience efficient TDUs from the 15th TP at the latest, with $\lambda > 0.5$. Indeed, in this set of models with $f_{env} = 0.0035$ and $f_{PDCZ} = 0.002$, we find that the models with $Z \leq 10^{-3}$ experience H ingestion TPs with peak H-burning luminosities reaching almost $10^{10} \, L_\odot$ (Table 2). The $Z = 0.02$ and 0.01 models also show marked increases in λ further along the TP-SAGB but in our simulations up to the 26th and 25th TPs, respectively, $\lambda < 0.5$ and no H ingestion events were encountered. An important implication of large λ values in SAGB stars is the narrowing (or disappearance) of the electron-capture SN channel due to a suppressed core growth rate.

The CBM parameter f_{env} (see Section 2.2) can be calibrated for the lower envelope convection boundaries during the TDU for low-mass AGB stars to reproduce the required partial mixing between the H-rich envelope and the ^{12}C-rich core to form a sufficiently large ^{13}C-pocket for the s-process. Lugaro et al. (2003) have proposed that a CBM parameter $f_{env} = 0.128$ would reproduce s-processobservables. However, Pignatari et al. (2013a) have shown that with $f_{env} = 0.126$ the galactic C-rich stars with the highest s-process enrichments are not reproduced (see e.g. Abia et al. 2002 and Zamora et al. 2009 for observations). The CBM at the bottom of the convective envelope during the TDU in high-mass AGB and SAGB stars leads to hot DUP (see Section 2.2). The appropriate value for f_{env} is not known for this situation, but numerical experiments show that adopting the same value that was calibrated to satisfy the constraints of a sufficiently sized ^{13}C-pocket in low-mass stars would lead to very intense H-burning that would lead to rapid disintegration of the AGB star (Herwig 2004a). In our benchmark model, we used a much smaller value of $f_{env} = 0.0035$. Generally speaking, a much smaller value for hot DUP compared to regular

TDU is justified because the energy released by burning protons mixed into the hot core will add buoyancy to the fluid elements which in turn will reduce the efficiency of the CBM process. While the efficiency of TDU depends only very weakly on f_{env} in low-mass AGB stars (Mowlavi 1999) this is entirely different when the DUP is hot. In this case the DUP efficiency is strongly dependent on f_{env}, as we will show in the following sections (see Fig. 8). The hot DUP, particularly with CBM, is a difficult phenomenon to simulate. Although it is approximated in our 1D code, the coupled behaviours of the burning and mixing together with the structural readjustment of the star following the peak He-shell flash luminosity is itself something that warrants further in-depth investigation (see also Herwig 2004).

3.3 Impact of CBM on the TP-SAGB phase and hydrogen-ingestion TPs

The efficiency and extent of CBM during the TP-SAGB is not known at present. There are little to no observational diagnostics that really help to constrain such mixing. It is thus important to study the impact of the choice of the e-folding lengths of the exponentially decaying diffusion coefficient ($f H_P$ in our CBM scheme) on the occurrence and behaviour of hydrogen ingestion events during the TP-SAGB. In order to accomplish this, we have computed a series of models from the end of the second DUP in our $7 \, M_\odot$ model with initial metallicity $Z = 10^{-4}$. We focus our study on the impact of two CBM parameters: f_{PDCZ} – the f value characterizing the mixing at the base of the PDCZ – and f_{env} – the equivalent value for the base of the convective envelope including during its penetration following the TP (TDU). The results of these models are summarized in
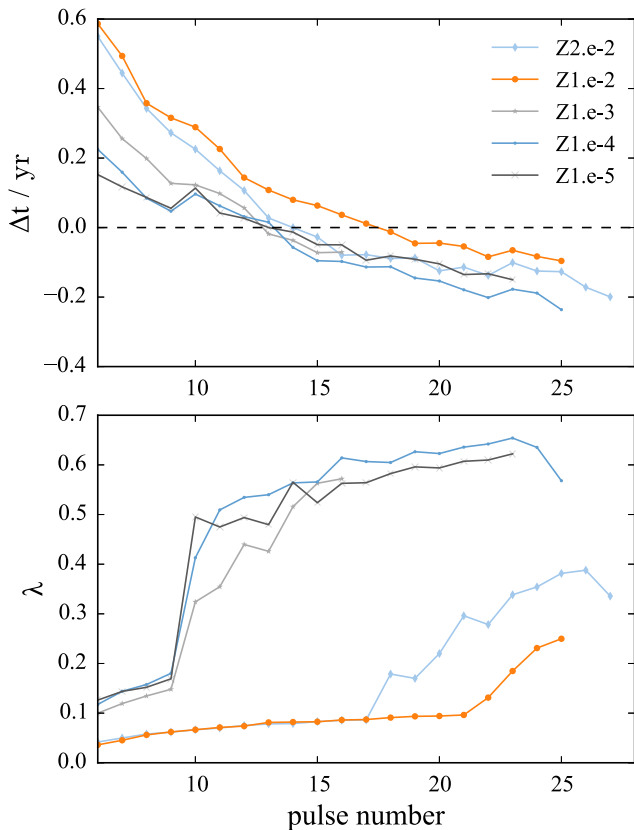
Figure 5. Top panel: time between the extinction of the PDCZ and the beginning of TDU, Δt (see Fig 4 and the text for details). Hence, above the horizontal dashed line at $\Delta t = 0$, the TDU begins after the extinction of the PDCZ and below the line $\Delta t = 0$ the TDU begins while the PDCZ is still active. Bottom panel: TDU efficiency λ – the ratio of the mass of material mixed up to the amount the H-free core grew during the preceding H-burning interpulse phase – as a function of pulse number for different metallicity models.

Table 3. Initially, we continued the computation of the model holding our original assumption for the CBM scheme ($f_{env} = 0.0035$, $f_{PDCZ} = 0.002$; see Section 2.2) and found that the model indeed encountered a situation whereby protons from the convective envelope were ingested into the PDCZ. This He-shell flash H ingestion is different than the equivalent event in low metallicity low- and

intermediate-mass stars (Fujimoto et al. 2000; Herwig 2003; Suda et al. 2004; Campbell & Lattanzio 2008; Cristallo et al. 2009a), or H-deficient post-AGB stars (Herwig et al. 2011). In those situations, the hydrogen-burning shell separating the hydrogen-rich and helium-rich material is either weak or completely inactive. The entropy barrier is thus weaker and it is easier for the PDCZ to ingest protons. In SAGB stars where DUP is hot (i.e. the hydrogen-burning shell is still active), it is much more difficult for the PDCZ to simply engulf some of the hydrogen-rich material in the same way. Instead, the combination of effects from the CBM below the PDCZ and the CBM below the convective envelope can be enough, in our current parametrizations, to initiate a convective-reactive event.

3.3.1 Fixed f_{env}

Fixing the value of f parameter at the base of the envelope at our original assumption of $f_{env} = 0.0035$ (see above), f_{PDCZ} was increased through the range 0.002–0.014. The impact on the TDU efficiency λ and the time between the onset of TDU and extinguishing of the PDCZ is shown in the bottom panel of Fig. 6. The peak He-burning luminosity during the shell flash is higher for larger values of f_{PDCZ}. As a result the TDU begins sooner (Fig. 6, top panel) and becomes more efficient (Fig. 6, bottom panel). All of the models in this series experience H ingestion during the TP-SAGB. Once this begins to occur, it becomes rather difficult to define at which point the PDCZ has extinguished. It is for this reason that only up to the 20th pulse is plotted in the top panel of Fig. 6.

The peak hydrogen-burning luminosity L_H is given for each model in Table 3 (first four entries). All of the models encounter at least one TP with $L_H > 10^9 \, L_\odot$ and in the case with the largest extent of CBM ($f_{PDCZ} = 0.014$) the H-burning luminosity even exceeds $10^{10} \, L_\odot$. That case is also unique because it is the only model in the series that mixes material up from the CO (He-free) core into the PDCZ during the He shell flash. This begins to happen at around pulse number 40. The C/O ratio for these four models as a function of evolutionary time is shown for the TP-SAGB phase in Fig. 7. The DUP efficiency is greater than unity for only the model with $f_{PDCZ} = 0.014$, indicating that for such a parametrization of the CBM below the PDCZ the CO core will not grow to the critical mass for electron-captures to trigger its collapse.

Table 3. Key properties of the models from the mixing parameter study at $Z = 10^{-4}$ with $M_{ini} = 7 \, M_\odot$. Aside from the models where no TPs occur, all of the models listed here experience H ingestion events. f_{PDCZ} is the CBM parameter f (equation 2) below the PDCZ and f_{env} is the parameter at the base of the convective envelope. The peak value of the H-burning luminosity is given in units of $10^9 \, L_\odot$ and whether the TDU efficiency λ is greater or less than unity is given in the final column.

| f_{PDCZ}	f_{env}	Comments on H ingestion events	peak $L_H / 10^9 \, L_\odot$	λ
0.002	0.0035		8.26	<1
0.004	0.0035		3.98	<1
0.008	0.0035		4.35	<1
0.014	0.0035	PDCZ mixes up some CO core.	17.4	>1
0.002	0.008		6.06	<1
0.002	0.014	Only 14 pulses computed.	3.87	>1
0.002	0.022	No TP. H shell corrosively burns into CO core.	–	–
0.004	0.008		7.47	<1
0.008	0.014	Only 13 pulses computed, PDCZ mixes up some CO core.	5.84	>1
0.014	0.014	Only 14 pulses computed, PDCZ mixes up some CO core; one pulse is shown in Fig. 9.	23.1	>1
0.014	0.022	No TP. H shell corrosively burns into CO core.	–	–
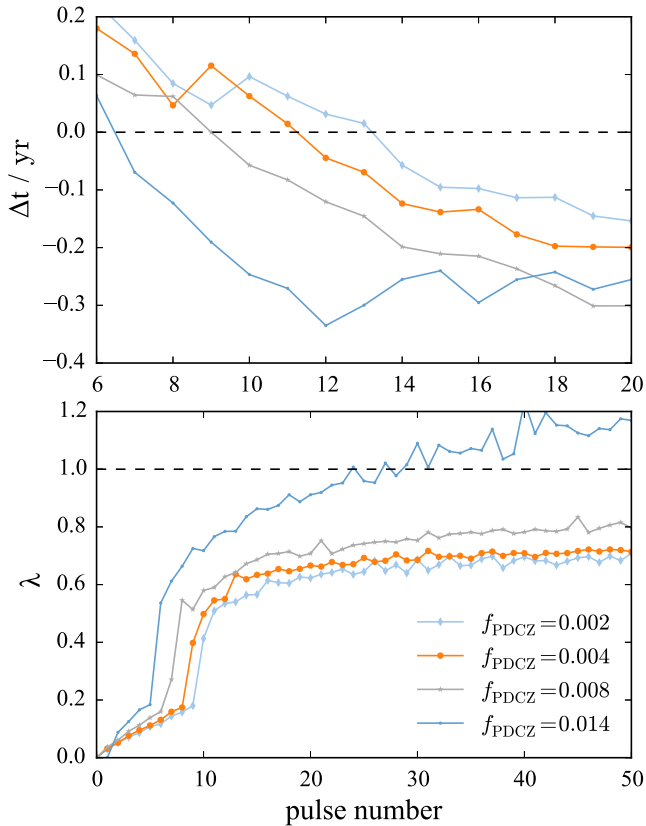
Figure 6. A series of models with $M = 7\,M_\odot$ and $Z = 10^{-4}$ in which $f_{env} = 0.0035$ and f_{PDCZ} is increased from 0.002 through 0.014 (first four entries in Table 3). Top panel: same as Fig. 5 (top panel). Bottom panel: same as Fig. 5 (bottom panel).
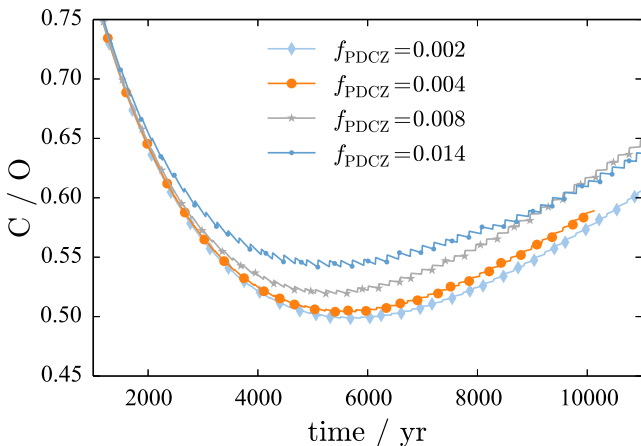

Figure 7. C/O ratio (C/O $= 16X(^{12}\text{C})/12X(^{16}\text{O})$) at the stellar surface for the series of models with $M = 7\,M_\odot$ and $Z = 10^{-4}$ in which $f_{env} = 0.0035$ and f_{PDCZ} is increased from 0.002 through 0.014 (first four models in Table 3).

3.3.2 Fixed f_{PDCZ}

A second series of models was computed in which we fixed the value of the f parameter below the PDCZ at our initial assumption of $f_{PDCZ} = 0.002$ and increased f_{env} through the range 0.0035–0.022. For the model with the largest value of the parameter ($f_{env} = 0.022$) no TPs were encountered. Instead the hydrogen-burning shell corrosively burned into the H-free core and, eventually, into the CO
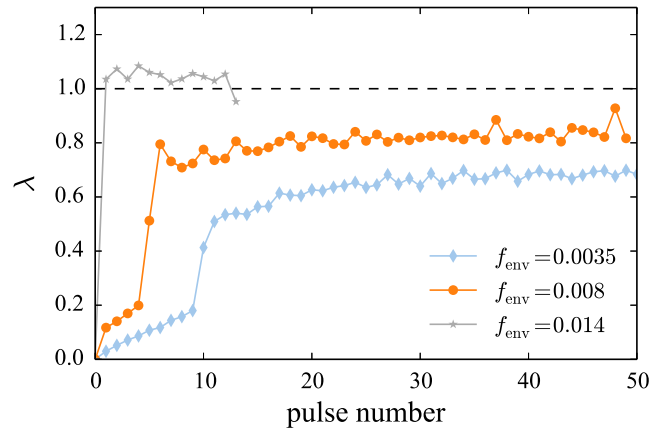

Figure 8. TDU efficiency λ for the series of models with $M = 7\,M_\odot$ and $Z = 10^{-4}$ in which $f_{PDCZ} = 0.002$ and f_{env} is increased from 0.0035 through 0.014 (first entry and middle three entries in Table 3). Model with $f_{env} = 0.022$ is actually not shown because it does not experience any TP events.

core (Herwig 2004a). With $f_{env} = 0.014$, hydrogen ingestion and efficient TDU with $\lambda > 1$ are found frequently from the second TP onwards (see Fig. 8). A summary of this series of models is provided in Table 3 (first entry and middle three entries).

3.3.3 Combined effect of f_{env} and f_{PDCZ}

In a final series of models, we increased both f_{PDCZ} and f_{env} in tandem (last four entries in Table 3). The models behave as predicted based on our individual parameter studies for each parameter. The combined effects of the CBM below the PDCZ and the hot-bottom burning H envelope cause the model to experience H ingestion TPs very early in the TP-SAGB phase (within the first 20 TPs). The model with $f_{env} = 0.014$ and $f_{PDCZ} = 0.014$ experiences the highest H-burning luminosity of all the models computed for this study: $2.31 \times 10^{10}\,L_\odot$. Fig. 9 shows a Kippenhahn (convective structure evolution) diagram of this most extreme H ingestion SAGB TP including contours of nuclear energy generation in the range 1– $10^{16}\,\text{erg}\,\text{g}^{-1}\,\text{s}^{-1}$ for the model with $f_{PDCZ} = 0.014$ and $f_{env} = 0.014$. The model predicts energy generation rates from hydrogen combustion in excess of $10^{15}\,\text{erg}\,\text{g}^{-1}\,\text{s}^{-1}$. The abundance profiles at this time are shown along with the temperature (top panel) and entropy (bottom panel) stratifications in Fig. 10. The model was computed for only 14 TPs, however the value of the *H*-number (equation 3) during the second TP in this case was $H \approx 1.1$. This suggests that the amount of energy being released in the ingestion event is likely at least 10 per cent greater than the internal energy of the material residing at the location where the energy is being released. If the CBM parameter choice is appropriate then the 1D hydrostatic stellar evolution assumptions are violated and the calculated results are indicative at best (see Section 4). For example, such strong energy release will certainly affect the hydrodynamic flow which will feed back into the ingestion event.

4 CONSEQUENCES OF HYDROGEN INGESTION DURING DREDGE-OUT AND THE TP-SAGB

We have identified in Section 3 two potential sites of H ingestion in SAGB stars and failed massive stars. These are stars that experience either dredge-out, He shell-flash TPs or both. In the dredge-out,
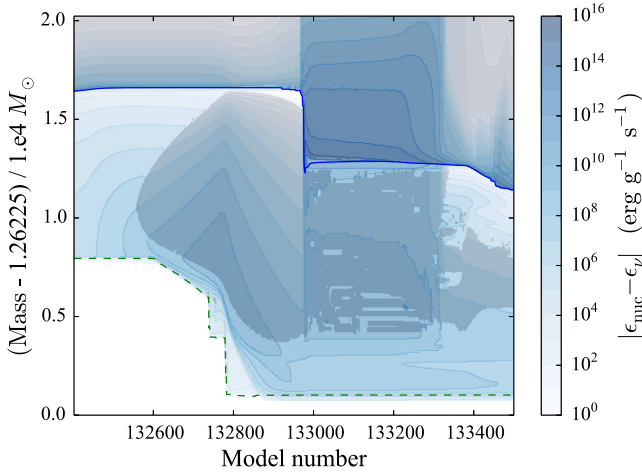
Figure 9. Evolution of the convective structure and nuclear energy generation during a TP in which hydrogen is ingested into the PDCZ. The model shown here had initial mass $7\,M_\odot$ and metallicity $Z = 10^{-4}$ and was computed with $f_{env} = 0.014$ and $f_{PDCZ} = 0.014$ (penultimate model in Table 3). The regions shaded in grey are convectively unstable and the blue contours show regions of nuclear energy generation. The solid blue line marks the boundary above which the mass fraction of hydrogen is greater than 10^{-6} and the dashed green line marks the edge of the CO core. The ingestion event occurs around model number 133000, at which time profile plots of the important quantities are given in Fig. 10.

the region of convective instability associated with the He-burning shell grows outwards in mass and eventually coalesces with the convective envelope. This allows for the transport of protons down to He-burning temperatures on a convective time-scale, where ^{12}C has been produced from He burning. Introducing protons to an environment rich in ^{12}C at temperatures of $\gtrsim 1.5 \times 10^8$ K results in a very rapid release of energy from H-^{12}C combustion (see also Gil-Pons & Doherty 2010).

Along the TP-SAGB, our models (assuming $f_{PDCZ} = 0.002$ and $f_{env} = 0.0035$; see Section 2) suggest that SAGB stars with a wide range of initial metallicities ($10^{-5} \leq Z \leq 0.02$) evolve towards the conditions required for an exchange of material between the PDCZ and the convective hydrogen envelope. Such a direction of evolution involves: (i) the shortening of the time between the end of the PDCZ and the onset of the TDU into the intershell and (ii) the increasing of the efficiency of the TDU, λ.

4.1 Validity of the 1D approximation

From our simulations of dredge-out in TP-SAGB stars – which are spherically symmetric models in hydrostatic equilibrium computed using the MESA code and holding the assumptions described in Section 2 – we have calculated the *H*-number (Equation 3) for the time when the H-^{12}C combustion is most energetic. This number is an estimation of the amount of energy released over one convective
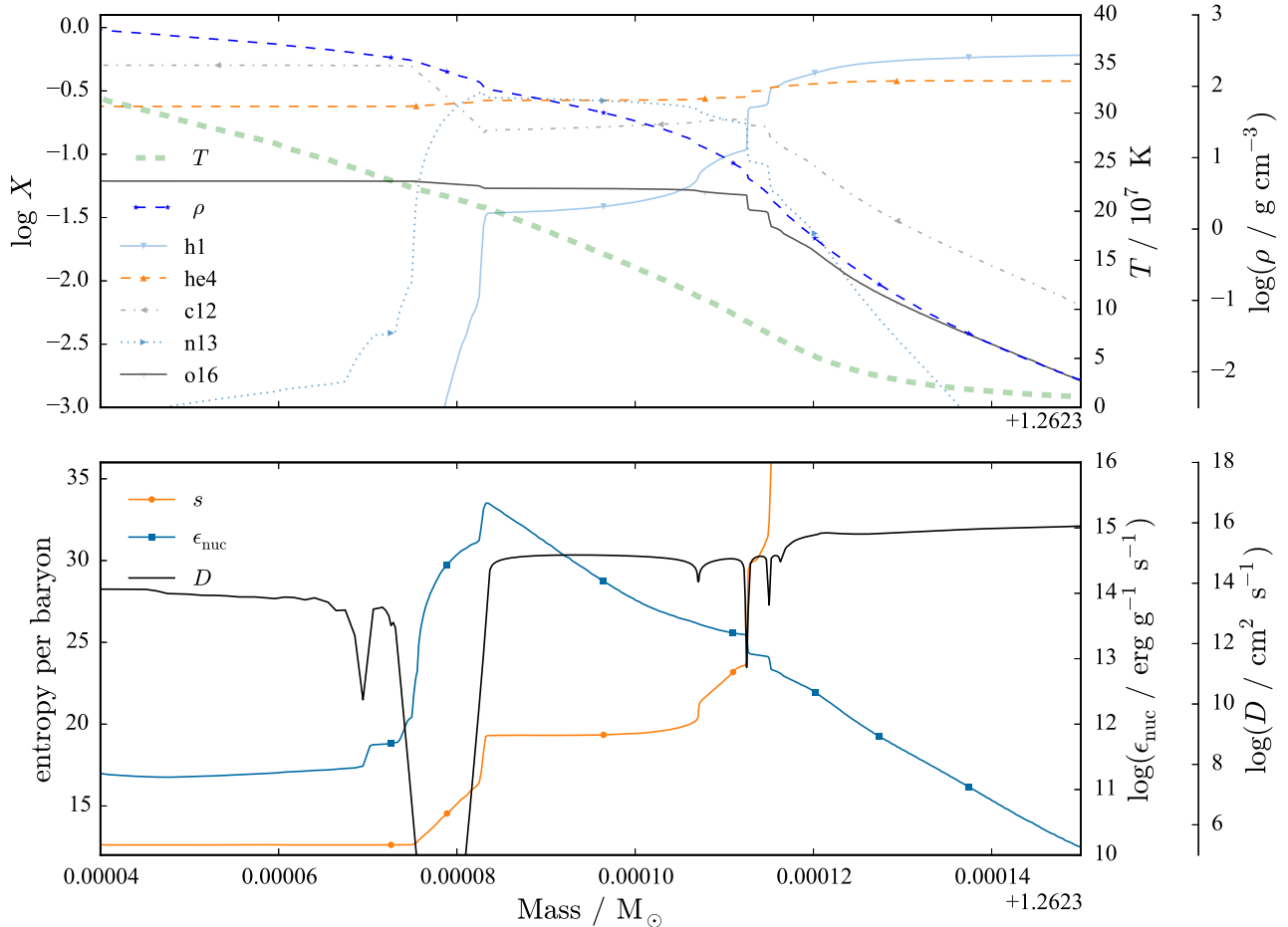
Figure 10. Abundance profiles, temperature and density (top panel) and entropy s, specific rate of nuclear energy generation and diffusion coefficient (bottom panel) in the $7\,M_\odot$ $Z = 10^{-4}$ model during the peak energy generation due to H-^{12}C combustion (around model 133000 in Fig. 9). In this model, the CBM parameters at the bottom of the PDCZ and at the bottom of the envelope were $f_{PDCZ} = 0.014$ and $f_{env} = 0.014$, respectively (see penultimate entry in Table 3).

turnover time-scale in units of the local internal energy of the stellar material. During dredge-out in an $8.4\,M_\odot$ stellar model with an initial metallicity of $Z = 0.01$ we find a lower limit of $H = 0.11$. During a TP of a $7\,M_\odot$ SAGB star model with an initial metallicity of $Z = 10^{-4}$ and CBM parameters $f_{PDCZ} = 0.002$ and $f_{env} = 0.014$ we estimate that $H \approx 1.1$. Such conditions will certainly feed back into the hydrodynamic flow of the stellar material, which in turn will feed back into the entrainment and burning rates (Herwig et al. 2014).

As we describe in Section 3, after some time in our 1D calculations the ingestion episode is quenched. This means that the flow of protons from the H-rich convective envelope into the convective He-burning layer is choked off by the formation of an entropy barrier. The formation of such an entropy barrier arises because the protons burn as they are diffused inwards, down towards higher temperatures. The time-scales of mixing, burning and nuclear energy generation are similar to one another. Under these conditions, it is questionable whether the MLT can provide the correct solution for the transport of entropy and nuclear species. The behaviour of H ingestion events would be characterized by: how many protons are mixed into the ^{12}C-rich layer, how far in are they transported and where is the energy from H-^{12}C combustion deposited. For this, 3D simulations are necessary (see e.g. Herwig et al. 2011, 2014; Stancliffe et al. 2011, for similar examples of H ingestion in low-metallicity AGB stars and post-AGB stars).

4.2 Mass ejection and transients triggered by proton-ingestion

The simulations by Herwig et al. (2014) suggest that H ingestion into ^{12}C-rich He-shell convection can trigger a non-radial instability, the GOSH. It is conceivable that a GOSH instability in a violent proton-ingestion event in an SAGB star could drive an outburst that rises through the star and is ejected in a pre-SN explosion. At the shell, temperatures can reach in excess of 2×10^8 K. These outbursts could have implications for multiple classes of 'supernova' explosions, both as precursors of narrow-line SNe and, as possible in explanations of specific peculiar subclasses of SNe. Although the thorough study needed to determine the viability of these outbursts in explaining these subclasses is beyond the scope of this paper, in this section we conduct a first look at the transient properties of these outbursts.

First and foremost, the mass ejecta from these outbursts can produce the circumstellar debris needed to explain Type IIn SNe. Observations of Type IIn SNe are providing a growing list of properties of the circumstellar medium surrounding these SN explosions (e.g. Miller et al. 2010; Kankare et al. 2012; Fox et al. 2013; Taddia et al. 2013; Moriya & Maeda 2014; Ofek et al. 2014). Ofek et al. (2014) argue that over half of all Type IIn SN have precursors within 1/3 yr of the SN explosion with masses exceeding 0.001 $M_\odot$. Moriya & Maeda (2014) instead argue that the IIn SNe in their sample are fit by enhanced mass loss rates of 10^{-3}–$1\,M_\odot$ yr^{-1} for 5–60 yr prior to the explosion with total ejecta masses lying between 0.01 and $10\,M_\odot$. Miller et al. (2010) argued that dense clumps exist as far out as 1.7×10^{16} cm. For most of these shell-burning outbursts, the explosion occurs too long before collapse to produce an observed signal in the SN light curve. However, in some cases, our models can produce the observed IIn circumstellar medium (CSM) distributions.

Corsi et al. (2014) and Gal-Yam et al. (2014) have seen evidence of outbursts at the few year time-frame even for SN not of the Type IIn subclass, the primary difference being the ejecta is smaller and the outburst happened longer prior to the SN explosion. These ex-
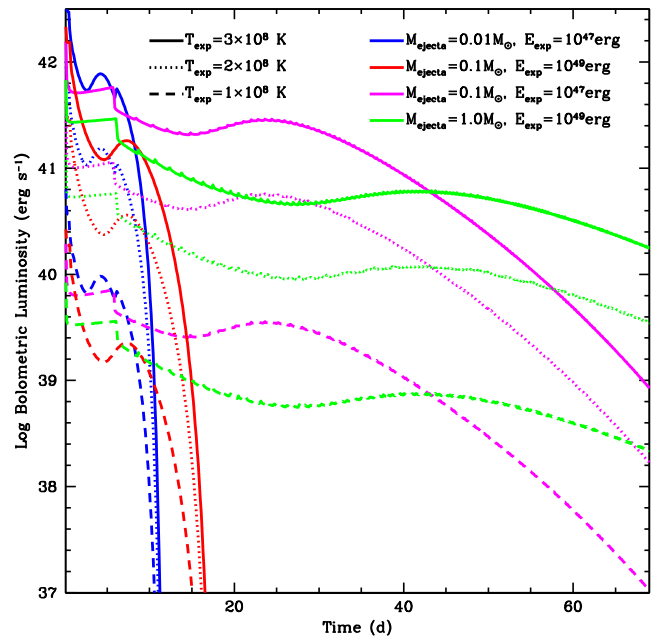

Figure 11. Bolometric light curves of the possible signature from violent shell-burning explosions for different combinations of the shell burning temperature, ejected mass and the energy imparted to the ejected mass.

plosions may also be an indicator of helium-shell proton-ingestion outbursts. To predict the shape of the light curve that could be produced during the ejection of material caused by a proton ingestion event occurring deep within the star, we mimic the outburst by assuming the hot material is ejected from the burning layer. As it rises through the star, it expands and cools adiabatically prior to bursting out of the stellar surface. We assume that the drive from the burning layer only allows the ejecta to expand laterally, and the volume of the ejecta increases as the square of its position until it is ejected from the star. Using the temperature at the burning layer, and assuming adiabatic expansion, we can calculate the thermal energy of the ejecta as it breaks out of the star.

After the outburst breaks out of the star, we use a semi-analytic solution to calculate the light curve of these explosions, assuming spherical symmetry and homologous outflow conditions (see Bayless et al. 2015, for details). To estimate the light curve of these outbursts, we varied the energy (10^{47}–10^{49} erg), temperature (1–3×10^8 K) and mass (0.01–0.1 $M_\odot$) of this rising outburst. Fig. 11 shows a range of light curves estimated from this method. The calculations assume average escape velocity v_{ejecta} set to $(2E_{exp}/M_{ejecta})^{1/2}$ where M_{ejecta} is the ejecta mass. The magnitude of the light curve depends sensitively on the thermal energy, but the duration of the burst can be altered by changing either the explosion energy or the mass, and without an accurate velocity measurement, it will be difficult to distinguish between these models.

Note that these outbursts lie somewhere between SNe and novae and, for both small ejecta masses ($<0.1\,M_\odot$) or energetic explosions, the duration is shorter than typical SNe with rise/decay times of the order of 10 d. Without more detailed calculations of the propagation of the burning episode through the star, it is difficult to constrain the light curve further. These light curves may explain the pre-explosion outbursts seen by Corsi et al. (2014) and Gal-Yam et al. (2014). Similar pre-SN outbursts and CSM production could be caused by the instability encountered in TP-SAGB stars

described by Lau et al. (2012), should the entire envelope not be ejected and the star recover and evolve to an electron-capture SN.

4.3 Neutron-capture nucleosynthesis and overabundance of n-capture products in ejected winds

H-^{12}C combustion produces ^{13}C, from which neutrons are then released via the ^{13}C(α, n)^{16}O reaction. Given the right conditions during the hydrogen-ingestion event (abundance of protons, abundance of ^{12}C and the temperature), intermediate neutron densities of $N_n \approx 10^{15}$ cm^{-3} can be produced, defined as the *i*-process by Cowan & Rose (1977, see Section 1).

i-process nucleosynthesis signatures are observed in young open clusters of the galactic disc (Mishenina et al. 2015) and may show up in galactic chemical evolution at lower metallicities, or in metal-poor mass-transfer binaries (Cristallo et al. 2009b; Lugaro et al. 2012b; Dardelet et al. 2015). If low-metallicity SAGB stars do indeed host the *i*-process, then the corresponding signature may be found in globular cluster stars with strongly He-rich (second) generations (Herwig et al. 2012; Charbonnel et al. 2013; Karakas et al. 2014; Shingles et al. 2015).

However, unless we have performed a three-dimensional hydrodynamic simulation-based analysis of the interaction of nuclear burning and convective fluid-dynamic flow, we cannot calculate the nucleosynthesis in the H-combustion DUP reliably based solely upon one-dimensional stellar evolution models (Herwig et al. 2011). In the meantime, we can explore a number of relevant questions that are independent of the hydrodynamic aspects. These are the enrichment of the envelope and ejecta of SAGB stars (which will be presented in this section) and the general properties of nucleosynthesis at *i*-process conditions. Dardelet et al. (2015) presented one-zone nucleosynthesis simulations for typical *i*-process conditions, i.e. neutron densities of $N_n \approx 10^{15}$cm^{-1}. They have shown that the abundance pattern of some C-enhanced metal-poor stars classified as CEMP-s/r stars (carrying simultaneously the signature of elements usually associated with *s*-process and those associated with *r*-process; Beers & Christlieb 2005; Masseron et al. 2010; Bisterzo et al. 2012; Lugaro et al. 2012a) can be remarkably well reproduced by one-zone simulations if the neutron exposure is used as a fitting parameter. If these preliminary results are confirmed in a more detailed investigation then H ingestion events in SAGB stars would be a possible site for the *i*-process observed in CEMP-s/r stars. The C enhancement in CEMP stars would then likely come from the C-rich He-shell layer of which a larger fraction would be mixed to the envelope and ejected during the violent non-radial instabilities associated with the H ingestion flash (Herwig et al. 2014) that are in contrast with 1D stellar evolution models. The predictions for *i*-process simulations rely on nuclear physics data that is presently only available from theory (Bertolli et al. 2013). Experiments for unstable species involved in *i*-process simulations will have to be performed in the future to improve this situation.

In order for *i*-process nucleosynthesis from the SAGB hydrogen-ingestion TPs to become observable, the nuclear production in the He-shell with H ingestion needs to be high enough, and repeated events are needed to enrich the envelope before it is lost to the interstellar medium. One concern would be that the intershell in the SAGB stars is so small in mass that even repeated exposure and DUP events may not lead to significant overabundances in the – at least initially – massive SAGB envelopes. One possible scenario mentioned above involves a dynamic ejection of envelope material triggered by the energy input and instabilities induced by the

H ingestion flash. Alternatively, in the TP-SAGB case the enrichment of the envelope may proceed more gradually, one DUP event at time.

Although the TDU in some cases can be efficient in terms of the DUP parameter ($\lambda \approx 1$; see Section 3.3 and Figs 6 and 8) the mass of the intershell region is only of the order of $\approx 10^{-4}$ M$_\odot$ (see Fig. 9). Even if large production factors can be regularly obtained in the intershell region, the large dilution into a massive SAGB envelope may prevent large overabundance factors in the ejected materials.

We have constructed a simple mixing model to clarify this question. In our simulation with $f_{env} = 0.014$, the core mass remains approximately constant due to efficient DUP after each TP. Thus, the total number of TPs that the model could encounter would depend only on the mass-loss rate for a given envelope mass. For $M_{env} = 6$ M$_\odot$ and an approximately constant interpulse time – because of the constant core mass with $\lambda \approx 1$ – of $t_{interp} \approx 782$ yr, a mass-loss rate of $\log(\dot{M}/\text{M}_\odot \text{ yr}^{-1}) = -5(-4)$ translates into about 800 (about 80) TPs. The overproduction factor can be estimated by evaluating the following simple mixing model:

$$s_{env}^{n+1} = s_{IS}^n \frac{f_{enr} m_{IS} + m_{env}^n}{m_{IS} + m_{env}} \tag{5}$$

$$m_{s,eject}^{n+1} = m_{s,eject}^n + s_{env}^{n+1} t_{interp} \dot{M} \tag{6}$$

$$m_{env}^{n+1} = m_{env}^n - t_{interp} \dot{M}, \tag{7}$$

where s_{env} and s_{IS} are the heavy element abundances in the envelope and in the intershell respectively, f_{enr} is the production factor of heavy elements in the intershell, m_{env} and m_{env} are the mass of the envelope and the intershell, respectively, $m_{s,eject}$ is the mass of heavy elements in the wind ejecta, and $\dot{M}$ is the mass-loss rate. The overabundance in the total wind ejecta is then $m_{s,eject}^{final}/m_{env}^{initial}$, and corresponds to [*s*/Fe] if *s* has the solar-scaled value in the initial abundance. This overabundance is shown in Fig. 12 as a function of assumed mass-loss rate and intershell production factors, assuming an average intershell mass of $m_{IS} = 7 \times 10^{-5}$ M$_\odot$ and an initial envelope mass of 6 M$_\odot$.

Some guidance on the expected production factors of the vigorous H ingestion/He-shell flash encountered in the SAGB TPs may be gained from the related situation in post-AGB H ingestion flash models representing Sakurai's object (Herwig et al. 2011). There, production factors of about 100 were found for an individual event, although limited to the first-peak elements. The initial metallicity of our simulation with $f_{env} = 0.014$ is $Z = 10^{-4}$ and therefore the production might be more efficient for heavier elements, since the neutron source is primary. Consistent with the lower initial abundances, the logarithmic production factors in the intershell may be in the range 3–3.5 after each H ingestion event (see marked range in Fig. 12).

We conclude that with an estimate of the SAGB mass-loss of $\log(\dot{M}/\text{M}_\odot \text{ yr}^{-1}) \approx -4.1$ and production factors of the order of 1000 in the intershell, we expect overabundances of the heavy *i*-process elements in the wind ejecta of 1–2 dex. Therefore, the *i*-process triggered by the ^{13}C(α, n)^{16}O reaction may have a comparable or even larger efficiency with respect to the ^{22}Ne neutron source activated at the bottom of the convective TPs (Doherty et al. 2014). On the other hand, the ^{13}C(α, n)^{16}O reaction is a much more efficient neutron source in producing heavier elements than ^{22}Ne(α, n)^{25}Mg. Indeed, the ^{22}Ne itself is also a relevant neutron poison and produces by the (α, n) channel another neutron poison in ^{25}Mg, reducing the neutron-capture efficiency beyond iron (see the behaviour of the ^{22}Ne as a neutron source in fast rotating massive
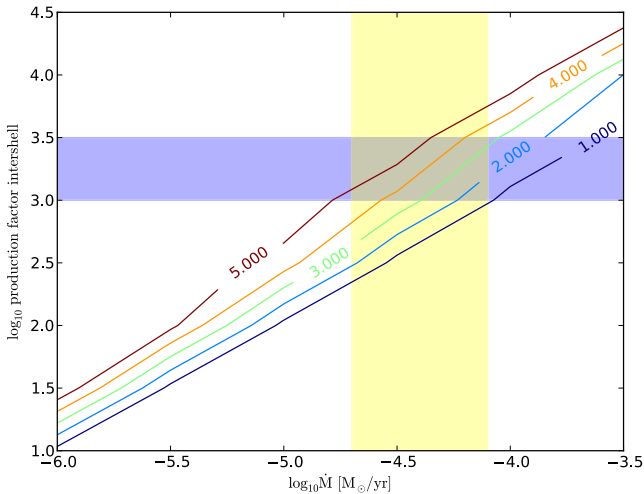
Figure 12. Estimate of n-capture overabundance in ejected winds of SAGB TP stars with H ingestion flash, as a function of stellar mass loss and n-capture production factor in the intershell. The lines are labelled with log of the overabundance in the ejecta; if the initial heavy element abundance was solar scaled, the labels would numerically correspond to [s/Fe] where s stands for the average of n-capture elements produced. The range of observed mass-loss rates in luminous M-type giants, supposedly massive AGB stars (van Loon et al. 2005) is shaded yellow. The n-capture production factor estimates (shown in blue, see text) are based on the detailed nucleosynthetic H ingestion flash investigation by Herwig et al. (2011), and our *i*-process single-zone calculations (Dardelet et al. 2015).

stars and in low-mass AGB stars at low metallicity, Husti et al. 2007; Pignatari et al. 2013b).

5 SUMMARY AND CONCLUSIONS

This paper describes two types of H ingestion events arising in simulations of 7–10 $M_\odot$ stars. One type of event occurs in our SAGB stellar evolution simulations during the TP phase and the other occurs during the dredge-out phase in SAGB stars and some stars that ignite neon off-centre.

Our simulations of SAGB stars with initial metallicities in the range $10^{-5} \le Z \le 0.02$ include CBM (Freytag et al. 1996; Herwig et al. 1997). All SAGB star models evolve during the TP phase towards conditions required for hydrogen-ingestion to occur during the He-shell flash. We suggest that this evolution is characterized by two main behaviours: (i) the efficiency of the penetration of the base of the convective envelope into the He intershell (TDU, see Section 3.2) increases as the stars evolve along the TP phase and (ii) the TDU begins before the PDCZ has completely extinguished.

Hydrogen-ingestion TPs occur in our SAGB stellar models for a large range of the CBM parameter f representing the mixing efficiency below the hydrogen envelope and below the PDCZ (f_{env} and f_{PDCZ}, respectively). In particular, using the value of $f_{PDCZ} = 0.008$ which has been shown to reproduce observational characteristics of post-AGB stars (Werner & Herwig 2006) and nova shell flashes (Denissenkov et al. 2013a), we find hydrogen-ingestion TPs to occur frequently for both $f_{env} = 0.0035$ and 0.014 (and for values in-between). It is important to stress that both of these values of f_{env} are much lower than what is usually assumed for AGB stars (see e.g. Lugaro et al. 2003). However, with DUP being hot in SAGB stars one would expect a greater entropy barrier at the bottom of the convective hydrogen envelope than in low-mass AGB stars and thus a lower efficiency of CBM. Quite what the efficiency of the CBM

is and hence, what an appropriate choice of the parameter f should be for the bottom of the convective envelope, is unclear at present. Our models suggest that for $f_{env} \gtrsim 0.014$ the efficiency of the 3DUP λ will be greater than unity and thus the He-free core will not grow during the TP-SAGB. This scenario would therefore suggest a very low electron-capture SN rate from SAGB stars (see also Poelarends et al. 2008).

The dredge-out phase in massive SAGB stars and some stars that ignite neon off-centre is another situation in which protons and ^{12}C are brought together under He-burning temperatures on a convective turnover time-scale (see also Ritossa et al. 1999; Siess 2007; Doherty et al. 2015). We have shown the results of a simulated dredge-out episode that indeed depicts precisely these conditions (see also Gil-Pons & Doherty 2010). The behaviour is less sensitive to CBM at the bottom of the convective hydrogen envelope in this scenario. Indeed, we have simulated the phenomenon by assuming no CBM takes place at all at this boundary and still the dredge-out occurs (in fact, several previously published SAGB stellar models depicting dredge-out do not include the effects of CBM, e.g. Siess 2007).

Our simulations are performed in spherical symmetry and employ MLT with time-dependent mixing treated as a diffusion process. Under these assumptions, the protons burn as they diffuse inwards and form an entropy barrier that chokes off further transport of hydrogen into the hot, ^{12}C-rich layers. Whether such a spherically symmetric entropy barrier would form in a real star and whether it would completely inhibit the transport of protons into the ^{12}C-rich layers is an open question. However, similar conditions have been found in simulations of the VLTP in Sakurai's object (Herwig et al. 2011). In that case observations can be explained if it is assumed that such a barrier formation and prohibition of proton transport does *not* occur.

The H-combustion events we find in our models are vigorous, leading to significant mixing events that bring together protons and ^{12}C at He-burning temperatures. Detailed nucleosynthesis simulations for a related case, Sakurai's object, suggest that substantial production of trans-iron elements would likely occur in such H ingestion events, and that the n-capture nucleosynthesis would proceed at a neutron density in-between that of the *s*-process and *r*-process (Herwig et al. 2011). The simulation of these *i*-process conditions for Sakurai's object indicate a strong production of the first-peak elements, while Ba and La are not efficiently made, leading to a simulated second to first peak *s*-process-index ratio of [hs/ls]≈ -1.8, roughly in agreement with observations. Post-AGB stars have only a very small amount of about 10^{-4} $M_\odot$ of H-rich envelope material left. This justified mixing assumptions that effectively limited the neutron exposure so that the observed abundance pattern of a large enhancement of first-peak but not second-peak elements could be reproduced.

In the H ingestion TPs of SAGB star models with CBM an envelope with several solar masses of H-rich material remains. This, as well as the higher neutron to Fe seed ratio in low-Z stars, and the possibility of recurrent H ingestion events in SAGB TPs imply that H ingestion events in SAGB stars could be a site for *i*-process with higher neutron exposure. This would lead to large enhancements of second-peak elements as observed in some of the CEMP-s/r stars. In fact, preliminary studies indicated that some CEMP-s/r stars are indeed very well reproduced by *i*-process-nucleosynthesis (Dardelet et al. 2015). We therefore propose that *i*-process in low-Z SAGB stars is a potential origin of some CEMP-s/r stars. Since hot bottom burning takes place in SAGB stars, their envelopes are O-rich and not C-rich. If H ingestion TP nucleosynthesis in SAGB stars

are responsible for a subset of the CEMP-s/r stars, the enrichment is probably coming from the ejection of intershell material during a dynamic response to the convective-reactive H ingestion flash, such as a GOSH (see Herwig et al. 2014 and Section 4.2). Such outbursts would produce faint transients lying somewhere between SNe and novae, and may explain a fraction of transient events that are observed shortly before a SN explosion.

REFERENCES

Abia C. et al., 2002, ApJ, 579, 817

Anderson A. J., 1997, PhD thesis, Univ. California, Berkeley

Angulo C. et al., 1999, Nucl. Phys. A, 656, 3

Bayless A. J., Even W., Frey L. H., Fryer C. L., Roming P. W. A., Young P. A., 2015, ApJ, 805, 98

Beers T. C., Christlieb N., 2005, ARA&A, 43, 531

Bertolli M. G., Herwig F., Pignatari M., Kawano T., 2013, preprint (arXiv:e-prints)

Bisterzo S., Gallino R., Straniero O., Cristallo S., Käppeler F., 2012, MN-RAS, 422, 849

Bisterzo S. et al., 2015, MNRAS, 449, 506

Blöcker T., 1995, A&A, 297, 727

Campbell S. W., Lattanzio J. C., 2008, A&A, 490, 769

Campbell S. W., Lugaro M., Karakas A. I., 2010, A&A, 522, L6

Casanova J., José J., García-Berro E., Calder A., Shore S. N., 2011, A&A, 527, A5

Caughlan G. R., Fowler W. A., 1988, At. Data Nucl. Data Tables, 40, 283

Charbonnel C., Chantereau W., Decressin T., Meynet G., Schaerer D., 2013, A&A, 557, L17

Chen M. C., Herwig F., Denissenkov P. A., Paxton B., 2014, MNRAS, 440, 1274

Corsi A. et al., 2014, ApJ, 782, 42

Cowan J. J., Rose W. K., 1977, ApJ, 212, 149

Cox J. P., Giuli R. T., 1968, in Cox J. P., Giuli R. T., eds, Principles of Stellar Structure. Gordon & Breach, New York

Cristallo S., Piersanti L., Straniero O., Gallino R., Domínguez I., Käppeler F., 2009a, PASA, 26, 139

Cristallo S., Straniero O., Gallino R., Piersanti L., Domínguez I., Lederer M. T., 2009b, ApJ, 696, 797

Dardelet L. et al., 2015, Proc. Sci., XIII Nuclei in the Cosmos. Debrecen, Hungary

Delgado-Inglada G., Rodríguez M., Peimbert M., Stasińska G., Morisset C., 2015, MNRAS, 449, 1797

Denissenkov P. A., Tout C. A., 2003, MNRAS, 340, 722

Denissenkov P. A., Herwig F., Bildsten L., Paxton B., 2013a, ApJ, 762, 8

Denissenkov P. A., Herwig F., Truran J. W., Paxton B., 2013b, ApJ, 772, 37

Denissenkov P. A., Truran J. W., Herwig F., Jones S., Paxton B., Nomoto K., Suzuki T., Toki H., 2015, MNRAS, 447, 2696

Deupree R. G., 2000, ApJ, 543, 395

Doherty C. L., Siess L., Lattanzio J. C., Gil-Pons P., 2010, MNRAS, 401, 1453

Doherty C. L., Gil-Pons P., Lau H. H. B., Lattanzio J. C., Siess L., 2014, MNRAS, 437, 195

Doherty C. L., Gil-Pons P., Siess L., Lattanzio J. C., Lau H. H. B., 2015, MNRAS, 446, 2599

Farmer R., Fields C. E., Timmes F. X., 2015, ApJ, 807, 184

Fox O. D., Filippenko A. V., Skrutskie M. F., Silverman J. M., Ganeshalingam M., Cenko S. B., Clubb K. I., 2013, AJ, 146, 2

Freytag B., Ludwig H. G., Steffen M., 1996, A&A, 313, 497

Fujimoto M. Y., Ikeda Y., Iben I. J., 2000, ApJ, 529, L25

Gal-Yam A. et al., 2014, Nature, 509, 471

Garcia-Berro E., Iben, Jr I., 1994, ApJ, 434, 306

Gil-Pons P., Doherty C. L., 2010, Mem. Soc. Astron. Ital., 81, 974

Glasner S. A., Livne E., Truran J. W., 2012, MNRAS, 427, 2411

Goriely S., Siess L., 2004, A&A, 421, L25

Herwig F., 2000, A&A, 360, 952

Herwig F., 2003, in Charbonnel C., Schaerer D., Meynet G., eds, ASP Conf. Ser. Vol. 304, CNO in the Universe. Astron. Soc. Pac., San Francisco, p. 318

Herwig F., 2004, ApJ, 605, 425

Herwig F., 2004a, ApJS, 155, 651

Herwig F., Blöcker T., Schönberner D. S., El Eid M. F., 1997, A&A, 324, L81

Herwig F., Blöcker T. B., Driebe T., 2000, in D'Antona F., Gallino R., eds, The Changes in Abundances in AGB stars. Memorie della Società Astronomia Italiana, 71, 745

Herwig F., Langer N., Lugaro M., 2003, ApJ, 593, 1056

Herwig F., Freytag B., Hueckstaedt R. M., Timmes F. X., 2006, ApJ, 642, 1057

Herwig F., Freytag B., Fuchs T., Hansen J. P., Hueckstaedt R. M., Porter D. H., Timmes F. X., Woodward P. R., 2007, in Kerschbaum F., Charbonnel C., Wing R. F., eds, ASP Conf. Ser. Vol. 378, Why Galaxies Care About AGB Stars: Their Importance as Actors and Probes. Astron. Soc. Pac., San Francisco, p. 43

Herwig F., Pignatari M., Woodward P. R., Porter D. H., Rockefeller G., Fryer C. L., Bennett M., Hirschi R., 2011, ApJ, 727, 89

Herwig F., VandenBerg D. A., Navarro J. F., Ferguson J., Paxton B., 2012, ApJ, 757, 132

Herwig F., Woodward P. R., Lin P.-H., Knox M., Fryer C., 2014, ApJ, 792, L3

Husti L., Gallino R., Bisterzo S., Cristallo S., Straniero O., 2007, Mem. Soc. Astron. Ital., 78, 523

Iglesias C. A., Rogers F. J., 1996, ApJ, 464, 943

Jones S. et al., 2013, ApJ, 772, 150

Kankare E. et al., 2012, MNRAS, 424, 855

Karakas A. I., Marino A. F., Nataf D. M., 2014, ApJ, 784, 32

Kromer M. et al., 2015, MNRAS, 450, 3045

Lau H. H. B., Gil-Pons P., Doherty C., Lattanzio J., 2012, A&A, 542, A1

Liu N., Gallino R., Bisterzo S., Davis A. M., Savina M. R., Pellin M. J., 2014, ApJ, 788, 163

Longland R., Iliadis C., Karakas A. I., 2012, Phys. Rev. C, 85, 065809

Lugaro M., Herwig F., Lattanzio J. C., Gallino R., Straniero O., 2003, ApJ, 586, 1305

Lugaro M., Campbell S. W., de Mink S. E., 2009, PASA, 26, 322

Lugaro M., Karakas A. I., Stancliffe R. J., Rijs C., 2012a, ApJ, 747, 2

Lugaro M., Karakas A. I., Stancliffe R. J., Rijs C., 2012b, in Kubono S., Hayakawa T., Kajino T., Miyatake H., Motobayashi T., Nomoto K., eds, AIP Conf. Proc. Vol. 1484, Origin of Matter and Evolution of Galaxies 2011. Am. Inst. Phys., New York, p. 111

Lugaro M., Tagliente G., Karakas A. I., Milazzo P. M., Käppeler F., Davis A. M., Savina M. R., 2014, ApJ, 780, 95

Masseron T., Johnson J. A., Plez B., Van Eck S., Primas F., Goriely S., Jorissen A., 2010, A&A, 509, A93

Mazzitelli I., D'Antona F., Ventura P., 1999, A&A, 348, 846

Meakin C. A., Arnett D., 2007, ApJ, 667, 448

Miller Bertolami M. M., Althaus L. G., Serenelli A. M., Panei J. A., 2006, A&A, 449, 313

Miller A. A. et al., 2010, MNRAS, 404, 305

Mishenina T. et al., 2015, MNRAS, 446, 3651

Mocák M., Müller E., Weiss A., Kifonidis K., 2009, A&A, 501, 659

Mocák M., Muller E., Siess L., 2011, A&A, 533, 53

Moriya T. J., Maeda K., 2014, ApJ, 790, L16
Mowlavi N., 1999, A&A, 344, 617
Nomoto K., 1984, ApJ, 277, 791
Nomoto K., 1987, ApJ, 322, 206
Ofek E. O. et al., 2014, ApJ, 789, 104
Paxton B., Bildsten L., Dotter A., Herwig F., Lesaffre P., Timmes F., 2011, ApJS, 192, 3
Paxton B. et al., 2013, ApJS, 208, 4
Paxton B. et al., 2015, ApJS, 220, 15
Piersanti L., Cristallo S., Straniero O., 2013, ApJ, 774, 98
Pignatari M. et al., 2013a, ApJS submitted preprint (arXiv:13076961)
Pignatari M. et al., 2013b, ApJ, 762, 31
Poelarends A. J. T., Herwig F., Langer N., Heger A., 2008, ApJ, 675, 614
Ribas I., Jordi C., Gimenez A., 2000, MNRAS, 318, L55
Ritossa C., García-Berro E., Iben, Jr, I., 1999, ApJ, 515, 381
Rogers T. M., Glatzmaier G. A., Jones C. A., 2006, ApJ, 653, 765
Schroder K.-P., Pols O. R., Eggleton P. P., 1997, MNRAS, 285, 696
Shingles L. J., Doherty C. L., Karakas A. I., Stancliffe R. J., Lattanzio J. C., Lugaro M., 2015, MNRAS, 452, 2804
Siess L., 2007, A&A, 476, 893
Siess L., 2010, A&A, 512, A10
Siess L., Goriely S., Langer N., 2004, A&A, 415, 1089
Stancliffe R. J., Dearborn D. S. P., Lattanzio J. C., Heap S. A., Campbell S. W., 2011, ApJ, 742, 121

Straniero O., Cristallo S., Piersanti L., 2014, ApJ, 785, 77
Suda T., Aikawa M., Machida M. N., Fujimoto M. Y., Iben I. J., 2004, ApJ, 611, 476
Taddia F. et al., 2013, A&A, 555, A10
Tian C.-L., Deng L.-C., Chan K.-L., 2009, MNRAS, 398, 1011
Tkachenko A. et al., 2014, MNRAS, 438, 3093
van Loon J. T., Cioni M.-R. L., Zijlstra A. A., Loup C., 2005, A&A, 438, 273
Ventura P., D'Antona F., 2011, MNRAS, 410, 2760
Weiss A., Ferguson J. W., 2009, A&A, 508, 1343
Werner K., Herwig F., 2006, PASP, 118, 183
Woodward P., Herwig F., Porter D., Fuchs T., Nowatzki A., Pignatari M., 2008, in O'Shea B. W., Heger A., eds, AIP Conf. Proc. Vol. 990, First Stars III: First Stars II Conference. Am. Inst. Phys., New York, p. 300
Woodward P. R., Herwig F., Lin P.-H., 2015, ApJ, 798, 49
Woosley S. E., Heger A., 2015, ApJ, 810, 34
Zamora O., Abia C., Plez B., Domínguez I., Cristallo S., 2009, A&A, 508, 909

This paper has been typeset from a TEX/LATEX file prepared by the author.